Colloids and Surfaces B: Biointerfaces 79 (2010) 467–479

Contents lists available at ScienceDirect

Colloids and Surfaces B: Biointerfaces

journal homepage: www.elsevier.com/locate/colsurfb

Molecular implications in the nanoencapsulation of the anti-tuberculosis drug rifampicin within flower-like polymeric micelles

Marcela A. Moretton[a,b], Romina J. Glisoni[a,b], Diego A. Chiappetta[a,b], Alejandro Sosnik[a,b,*]

[a] The Group of Biomaterials and Nanotechnology for Improved Medicines (BIONIMED), Department of Pharmaceutical Technology, Faculty of Pharmacy and Biochemistry, University of Buenos Aires, Buenos Aires CP1113, Argentina
[b] National Science Research Council (CONICET), Buenos Aires, Argentina

ARTICLE INFO

Article history:
Received 28 January 2010
Received in revised form 4 May 2010
Accepted 4 May 2010
Available online 12 May 2010

Keywords:
Microwave-Assisted Polymer Synthesis (MAPS)
Poly(epsilon-caprolactone)-*b*-poly(ethylene glycol)-poly(epsilon-caprolactone) block copolymers
Flower-like polymeric micelles
Tuberculosis
Rifampicin encapsulation

ABSTRACT

Tuberculosis (TB) is the second most deadly infectious disease behind the Human Immunodeficiency Virus (HIV). An effective pharmacotherapy has been available for more than 5 decades. However, the length of the treatment and the pill burden result in low patient compliance and adherence to the regimens. Nanotechnologies can overcome these basic technological drawbacks. The present work explored the molecular implications governing the encapsulation and water solubilization of RIF within flower-like micelles of poly(epsilon-caprolactone)-*b*-poly(ethylene glycol)-poly(epsilon-caprolactone) (PCL-PEG-PCL) block copolymers. Ten derivatives of different molecular weight and hydrophobic/hydrophilic caprolactone/ethylene oxide ratio (CL/EO) were synthesized by a fast and high-yield Microwave-Assisted Polymer Synthesis (MAPS) technique; CL/EO values are determined by taking the ratios of the number of repeating units in the PCL and the PEG segments. The aggregation behavior of the copolymers was thoroughly investigated by means of surface tension (critical micellar concentration), dynamic light scattering (size, size distribution and zeta potential) and transmission electron microscopy (morphology). In general, the greater the central PEG segment, the larger the micelles formed. The physical stability was intimately associated with the molecular weight and the composition. Then, the encapsulation of RIF in the different copolymer families was evaluated, and the physical stability of the drug-loaded aggregates characterized. The micellar size appears as the most crucial property, this phenomenon being primarily controlled by the molecular weight of the PEG central block. Having expressed this, sufficiently high CL/EO ratios (and long PCL segments) are also demanded to attain stable micellar systems with cores that are large enough to host the bulky RIF molecule.

1. Introduction

Tuberculosis (TB) is a deadly infectious disease and one of the main challenges in public health [1]. Approximately 2 billion people are currently infected with *Mycobacterium tuberculosis* [2], though only those living under deficient sanitary and nutritional conditions usually present a high risk of developing the active disease (see below). TB primarily affects the respiratory system, though in the absence of an effective chemotherapy, highly aggressive extrapulmonary forms of the disease appear at later stages [3,4]. TB is the second most deadly infection behind the Human Immunodeficiency Virus (HIV) [5]. According to the World Health Organization (WHO), every year more than 9 million people are newly infected; 5–10% of them develop the active disease. The annual mortality toll is approximately 1.7 million people [6]. TB is endemic in developing countries and has resurged in developed ones associated with HIV [7]. It is worth mentioning that HIV-infected patients are more prone to develop active TB, with levels of approximately 50–60%. Due to the high prevalence of HIV/TB co-infection, the WHO declared the global sanitary emergency in 1993 [8].

The standard first-line pharmacotherapy comprises a first stage (2 months) combining rifampicin (RIF), isoniazide (INH), pyrazinamide and ethambutol and a second one (4 months) with only RIF and INH [9,10]. Prolonged treatments and pill burden result in low patient compliance and low adherence levels to the regimens. Treatment interruption is the main cause of therapeutic failure and development of multidrug resistant TB (MDR-TB) [11]. TB remains the most important cause of preventable deaths [12].

RIF, one the most potent and effective anti-TB agents [13], is a high molecular weight (822.95 Da) amphoteric molecule with pK_{a1}

* Corresponding author at: Department of Pharmaceutical Technology, Faculty of Pharmacy and Biochemistry, University of Buenos Aires, 956 Junín St., 6th Floor, Buenos Aires CP1113, Argentina. Tel.: +54 11 4964 8273; fax: +54 11 4964 8273.
E-mail address: alesosnik@gmail.com (A. Sosnik).

0927-7765/$ – see front matter © 2010 Elsevier B.V. All rights reserved.
doi:10.1016/j.colsurfb.2010.05.016

and pK_{a2} values of 1.7 and 7.9 for the aromatic 4-hydroxyl group and the 3-piperazine nitrogen, respectively [14]; the isoelectric point is 4.8. The intrinsic solubility fluctuates from 1 to 3 mg/mL at pH values between 3 and 7.4 [15]. RIF is also amphiphilic [16]. According to the Biopharmaceutic Classification System (BCS), RIF is classified into Class II drugs (low aqueous solubility and high permeability) [17]. However, its reclassification into Class IV (low aqueous solubility and low permeability) has been more recently recommended [18]. In the stomach, RIF is hydrolyzed to 3-formyl rifampicin SV (F-RIF), a form that does not show activity *in vivo* due to an extremely low intestinal absorption. The acid degradation is significantly fastened by the presence of INH [19,20]; RIF/INH co-administration (e.g., fixed dose combinations, FDC) is frequently employed to prevent monotherapy that leads to the development of resistance [21]. This deleterious interaction is often neglected by clinicians who still recommend this practice. WHO has expressed its concern due to the relatively low oral bioavailability of RIF co-administered with INH [22]. Under basic pH conditions (>7.4), RIF undergoes oxidation [23] or desacetylation [24]. RIF is relatively stable under neutral pH.

To improve its aqueous solubility, RIF has been complexed with cyclodextrins (CD) [25–27]; solubility increased up to 3-fold. Another approach was the complexation with pristine and mannosylated 5th generation poly(propyleneimine) dendrimers [28]. Mannosylation reduced the solubilization capability of the dendrimer from 52 (20-fold) to 5 mg/mL (2-fold).

Encapsulation within polymeric micelles has become one of the most attractive and well-investigated nanotechnologies to enhance the water solubility and stability of poorly water soluble and instable drugs [29]. Poly(ethylene oxide)-*b*-poly(propylene oxide)-poly(ethylene oxide) (PEO-PPO-PEO) copolymers [30,31] and poly(epsilon-caprolactone)-*b*-poly(ethylene glycol)-poly(epsilon-caprolactone) (PCL-PEG-PCL) [32,33] are among the most popular micelle-forming biomaterials. Surprisingly, the encapsulation of RIF in polymeric micelles has not been previously reported.

As a strategy to stabilize RIF towards its administration by the oral route under gastric pH conditions and in the presence of INH, preliminary studies investigated its encapsulation within micelles of linear and branched PEO-PPO derivatives with a broad spectrum of molecular weights and hydrophilic/lipophilic balances [34]. However, the drug was not incorporated into the micelles, most likely due to their inability to host this extremely bulky molecule. These results stressed the complexity of the encapsulation process of RIF.

Flower-like micelles are formed by the aggregation of amphiphile ABA triblock copolymers that combine two terminal hydrophobic A segments with a central hydrophilic B one [32,33]. The looped hydrophilic corona often confers the aggregate higher physical stability than conventional star-like micelles generated by AB diblocks and BAB triblocks [35], and presumably leads to larger nanostructures.

The present work explored the molecular implications governing the encapsulation and apparent water-solubilization of RIF within micelles of PCL-PEG-PCL block copolymers as a nanotechnological approach to stabilize the drug towards its administration by the oral route. Ten derivatives of different molecular weight and PCL/PEG hydrophobic/hydrophilic balance were synthesized by a fast and high-yield Microwave-Assisted Polymer Synthesis (MAPS) technique [36]. The aggregation behavior of the copolymers was thoroughly investigated by means of surface tension, dynamic light scattering and transmission electron microscopy. Then, the encapsulation of RIF in the different copolymer families was evaluated, and the physical stability of the drug-loaded aggregates fully characterized. Our findings strongly support that the micellar size is the key parameter governing the encapsulation of RIF in polymeric micelles.

2. Materials and methods

2.1. Materials

Poly(ethylene glycol) of molecular weights 6000 Da (PEG6000), 10,000 Da (PEG10000) and 20,000 Da (PEG20000) were provided by Merck Chemicals (Buenos Aires, Argentina) and were dried under vacuum (100–120 °C in oil bath, 2 h) before use. Monomethoxy-poly(ethylene glycol) of molecular weight 5000 Da (MPEG5000, Sigma, St Louis, MO, USA) was used to synthesize an MPEG-PCL diblock. Epsilon-caprolactone 99% (monomer, CL, Sigma), tin(II) 2-ethylhexanoate 95% (catalyst, SnOct, Sigma), rifampicin 98.2% (Parafarm®, Buenos Aires, Argentina) and solvents of analytical grade were used as received.

2.2. Copolymer synthesis

The apparatus used for polymerization was a household microwave oven (Itedo™, radiation frequency 2.45 GHz, potency 800W, China) with ten power levels. Conventional ovens graduate the irradiation power by means of "on/off" cycles of the magnetron (pulsed irradiation) [37]. Basically, the potency is maintained constant at 800W though the duration of the "on" and "off" periods is modified according to the power level employed. The oven was adapted to enable the connection of a condenser. The different PCL-PEG-PCL triblocks were synthesized by a ring-opening polymerization reaction (ROP) catalyzed by SnOct. The synthetic procedure is exemplified hereby for a copolymer of PEG10000 containing in average two terminal PCL segments with a molecular weight of 4500 Da (approximately 40 CL units/arm). This copolymer is denoted as 4500–10000–4500. Briefly, PEG10000 (20.1 g, 2×10^{-3} mol) was poured into a 250 mL round-bottom flask and dried as described above. Then, epsilon-caprolactone (21.1 g, 0.185 mol, 10% in molar excess) and SnOct (1.87 g, 4.6×10^{-3} mol, 1/40 molar ratio to CL) were added, and the round-bottom flask was placed in the center of the microwave oven and connected to the condenser. The reaction mixture was exposed to microwave radiation for: (i) 1 min at power 5, (ii) 10 min at power 3 and (iii) 4 min at power 5. The total reaction time was 15 min. To overcome the high viscosity of PEG20000 and the inefficient mixing of the reagents, the dry PEG was primarily dissolved in dimethylformamide (DMF, 30% w/v final PEG concentration) and, only then, the monomer and the catalyst were added and mixed. To prevent DMF overheating and solvent loss, the radiation pattern was slightly modified: (i) 1 min at power 3 and (ii) 14 min at power 2. The total reaction time was 15 min, under reflux. To isolate the product, the crude was dissolved in dichloromethane (50 mL) and precipitated in petroleum ether 40–60° or *n*-heptane (500 mL). The cleaning procedure was repeated one more time for PEG6000 and PEG10000 and twice for PEG20000 copolymers (to remove DMF residues), respectively. The product was isolated by filtration, washed several times with petroleum ether 40–60°, dried until constant weight at room temperature and stored at −20 °C until use. By varying the molecular weight of the PEG initiator and the CL/PEG feeding ratio, PCL blocks of different lengths were produced. In general, white to yellowish solids were obtained.

2.3. Copolymer characterization

Proton nuclear magnetic resonance (^{1}H NMR) spectra were obtained from deuterated chloroform (Sigma) solutions at room temperature on a Bruker MSL300 spectrometer (Karlsruhe, Germany), at 300 MHz. The hydrophobic/hydrophilic balance, as represented by the CL/EO molar ratio, and the number-average molecular weight (M_n) of the different copolymers were calculated

by rationing the integration area of the peaks of PCL protons (2H, triplet, 2.30 ppm) and PEG (4H, multiplet, 3.65 ppm).

Fourier transform infrared (FT-IR) spectra were recorded in an FT-IR Spectrophotometer (PerkinElmer One, Waltham, MA, USA) using KBr windows.

Number- and weight-average molecular weights (M_n and M_w) and molecular weight distributions (M_w/M_n polydispersity, PDI) were determined by gel permeation chromatography (GPC) using a Knaüer GPC instrument (Berlin, Germany) provided with a refractive index detector. A set of 50 Å, 100 Å and M2 (Phenomenex Inc., Torrance, CA, USA) and 104 Å (Waters, Inc., Milford, MA, USA) columns ultrastiragel column, conditioned at 25 °C was used to elute samples at 1 mL/min HPLC-grade tetrahydrofuran flow rate. Polystyrene standards (Polymer Laboratories, Shropshire, UK) were used for calibration.

2.4. Thermal analysis of the copolymers in bulk

The thermal behavior of the different copolymers was characterized by differential scanning calorimetry (DSC, Mettler Toledo TA-400 differential scanning calorimeter, Columbus, OH, USA). To erase their thermal history and enable reliable comparisons among the different copolymers, samples were heated at 100 °C (1 h) and cooled to 25 °C (14 ± 0.5 °C/h). Then, copolymers (4–7 mg) were sealed in 40 μL Al-cruicible pans and heated from 25 °C to 100 °C at 5 °C/min under nitrogen atmosphere. PEG initiators were analyzed for comparison. The melting temperature (T_m) and the normalized enthalpy of fusion (ΔH_m) were determined.

2.5. Copolymer solubility in water

Copolymer solubility was determined by gravimetric analysis. Increasing copolymer amounts were solubilized in acetone (11 mL) and added (drop wise, 20 min) to water (10 mL) under mechanical stirring (three-blade propeller, 1060 RPM) at room temperature. Stirring was continued for 1 h to enable the total evaporation of the acetone (see below) and samples were filtered (0.45 μm, cellulose nitrate membranes, Whatman® GmbH, Dassel, Germany) to remove insoluble copolymer. To determine the solubility of the copolymers in water, 1 mL solution was poured into a weighed vial, dried in a vacuum oven at 45 °C until constant weight and the dry copolymer re-weighed. Percentages of solubility (%) were calculated by difference and expressed as mean ±S.D. ($n = 3$).

2.6. Preparation of RIF-free and RIF-loaded PCL-PEG-PCL micelles

RIF (in slight excess, approximately 15 mg/mL) and the corresponding copolymer were co-solubilized in acetone (11 mL) and added drop wise to water (10 mL) under mechanical stirring (three-blade propeller, 1060 RPM) using a programmable syringe infusion pump (PC11UB, APEMA, Argentina). Four addition times were preliminary evaluated by adjusting the flow in the infusion device: (i) 10, (ii) 20, (iii) 30 and (iv) 40 min. Mechanical stirring was continued for 1 h (until total acetone evaporation, see below) and filtered (0.45 μm cellulose nitrate membranes) to remove insoluble RIF and copolymer. To prepare drug-free micelles, a similar procedure was followed, though without the addition of drug in the first step. To assure the total elimination of the organic solvent, acetone contents were determined at different time points by Gas Chromatography (GC Hewlett Packard 6890, Palo Alto, CA, USA) with column Alltech Heliflex AT-Wax (length: 30 m, i.d.: 0.25 mm, Alltech Associates, Inc., Deerfield, IL, USA) using He as carrier (flow of 1 Kg/cm^2). The temperature of the oven, the injector and the detector was 40 °C. Each sample (1 μL) was analyzed by duplicate. Results indicated that after 1 h of mechanical stirring the concentration of acetone was <100 ppm; the maximal level specified by the European Pharmacopeia for pharmaceutical formulations is 5000 ppm [38]. Thus, samples were considered acetone-free after 1 h. To determine the concentration of RIF in the different micellar systems, RIF-loaded samples (1 mL) were dried under vacuum and dissolved in DMF. RIF concentrations were determined by UV (340 nm, CARY [1E] UV–Visible Spectrophotometer Varian, Palo Alto, CA, USA) at 25 °C using a calibration curve of RIF solutions in DMF covering the range between 5.5 and 33.2 μg/mL (correlation factor was 0.9995–0.9999). UV is a sensitive method for RIF, though it cannot be used in studies where the chemical stability of RIF is compromised, as degradation products show similar absorption patterns [19,39]. RIF does not undergo degradation under the neutral conditions of the encapsulation process employed, thus UV appears as a reliable method of analysis. Polymer solutions in DMF were used as blank. RIF concentrations in the different micellar systems are expressed in mg/mL as the mean ±S.D. ($n = 3$). Solubility factors (f_s) were calculated according to the equation:

$$f_s = \frac{S_a}{S_{water}},$$

S_a and S_{water} being the apparent solubility of RIF in the micellar system and the intrinsic solubility in copolymer-free distilled water (2.56 mg/mL, pH 5.8).

To evaluate the physical stability of RIF-loaded micelles, samples were incubated at 25 °C and the drug concentration monitored over 1 week according to the procedure depicted above. Statistical differences ($p < 0.05$) of S_a at a certain time point with respect to the initial value were analyzed using the Dunnett's Multiple Comparison Test.

2.7. Measurement of the critical micellar concentration (CMC)

The CMC of each copolymer was determined by means of surface tension using the du Noüy ring method (Fernández Berlusconi y Rocca SRL, Buenos Aires, Argentina), at 18 ± 0.5 °C. To express the results in molar (M), the M_n value determined by ^{1}H NMR was used. Experiments were carried out in triplicates and results expressed as the mean value.

2.8. Measurement of micellar size, size distribution and zeta potential

The size, size distribution and zeta potential of drug-free and drug-loaded micelles were measured by Dynamic Light Scattering (DLS, Zetasizer Nano-Zs, Malvern Instruments, Worcestershire, UK) provided with a 4 mW He–Ne (633 nm) laser and a digital correlator ZEN3600, at 25 °C. Measurements were conducted at a scattering angle $\theta = 173°$ to the incident beam. Samples were prepared in MilliQ water, filtered by clarifying filters (0.45 μm, cellulose nitrate) and equilibrated at 25 °C for at least 30 min prior to the analysis. Data were analyzed using CONTIN algorithms (Malvern Instruments). Results of hydrodynamic diameter (d_h) and polydispersity index (PDI) are expressed as the average of at least three measurements. To evaluate the physical stability of the systems, drug-free and drug-loaded samples were incubated at 25 °C and the same parameters monitored over 1 week.

2.9. Visualization of drug-free and drug-containing micelles

The morphology of drug-free and RIF-loaded 4% PCL3700-PEG10000-PCL3700 micelles was studied by means of transmission electron microscopy (Philips CM-12 TEM apparatus, FEI Company, Eindhoven, The Netherlands). Samples (5 μL) were placed onto a grid covered with Fomvar film. After 30 s, the excess was carefully removed with filter paper and uranyl acetate (2% w/v, 5 μl) was added. After 30 s, the excess was removed and water (5 μL) was

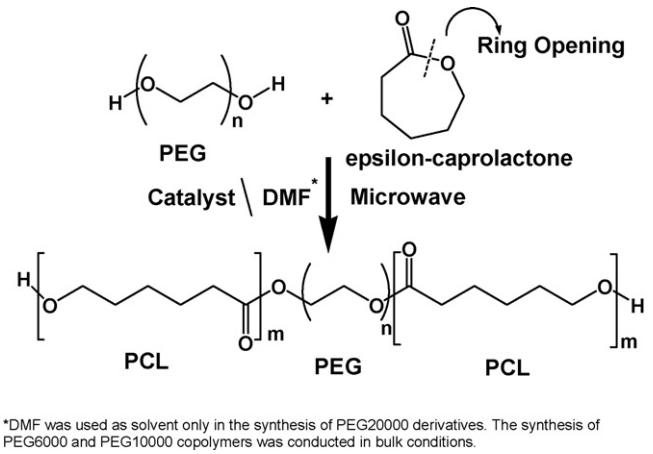

Fig. 1. Microwave-assisted ring-opening polymerization reaction of PCL–PEG–PCL block copolymers.

added, left for 30 s and removed. Samples were finally dried in a closed container with silicagel and analyzed. The diameter of the micelles/aggregates was measured using a calibrated scale.

3. Results and discussion

3.1. Copolymer synthesis and characterization

To investigate the molecular implications influencing the encapsulation of RIF within flower-like polymeric micelles, three families of PCL-PEG-PCL amphiphiles were synthesized by the ROP of epsilon-caprolactone initiated by poly(ethylene glycol) precursors of different molecular weight (PEG6000, PEG10000 and PEG20000) in the presence of SnOct (Fig. 1); this catalyst has been approved by the US FDA for use in biomedical devices [40]. Copolymers display gradual compositional changes in (i) the molecular weight of the central PEG block, (ii) the molecular weight of the copolymer, (iii) the CL/EO ratio and (iv) the length of the PCL terminal blocks. The common thermally driven synthetic technique [41] was replaced by a microwave-assisted one [36]. Main features of this technology are (i) shorter reaction times, (ii) higher yields, (iii) limited generation of by-products, and, due to radiation homogenously distributed, (iv) the relatively easy scale-up without detrimental effects [37]. Thus, MAPS appears as a very appealing approach for the synthesis of polymers for (bio)pharmaceutical applications. Depending on the molecular weight of PEG, reactions were conducted in bulk or solvent conditions. Reaction times were substantially shorter (15 min as opposed to 2.5 h [41]) and yields were greater than 95%. The main molecular properties of the different derivatives are summarized in Table 1.

Table 2
DSC data of the different PCL–PEG–PCL amphiphiles synthesized by MAPS. PEG precursors are included for comparison.

PCL–PEG–PCL copolymer	T_m (°C)	ΔH_m (J/g)
PEG6000	63	214.8
1050–6000–1050	54	122.4
1450–6000–1450	52	124.2
2550–6000–2550	54	111.0
PEG10000	60	191.7
1300–10000–1300	59	134.0
2600–10000–2600	57	113.8
3700–10000–3700	58	113.4
4500–10000–4500	56	110.2
PEG20000	64	184.2
1500–20000–1500	58	136.5
3800–20000–3800	58	131.7
7850–20000–7850	56	121.0

Experimental CL/EO and M_n values were determined from ^{1}H NMR spectra. Findings were in good agreement with the theoretical composition and confirmed the high monomer conversion. GPC analysis revealed the presence of unimodal molecular weight distributions and relatively low polydispersity (PDI) values (<1.38). Deviations of GPC data from M_n values calculated by ^{1}H NMR (especially for PEG20000 copolymers) could stem from the fact that the standards used were of polystyrene. FT-IR analysis showed the strong band of ester carbonyl streching at 1725 cm^{-1} that is characteristic of PCL [41].

3.2. Thermal analysis of the copolymers in bulk

The generation of physically stable micelles depends on the crystallization of PCL blocks in the micellar core; micelles with amorphous PCL blocks are more prone to undergo size growth over time due to fusion with PCL blocks belonging to other copolymer molecules in other aggregates (see below). To characterize the thermal behavior of the copolymers in the bulk, samples were analyzed by DSC (Table 2). Pristine PEG precursors show T_m in the range between 60 and 64 °C [42]. A gradual increase in the molecular weight resulted in a decrease of ΔH_m. Incorporation of PCL segments affected the crystallizability of PEG and led to a gradual decrease in both T_m and ΔH_m of PEG. The longer the PCL segment, the more pronounced the detrimental effect. This phenomenon was more notorious for short PEG blocks (Table 2); e.g., T_m and ΔH_m decreased from 63 °C and 214.8 J/g for PEG6000 to 54 °C and 111.0 J/g for 2550–6000–2550, representing 48% decrease in the degree of crystallinity. These findings indicated a mild to strong detrimental effect of PCL segments on the crystallization of PEG central blocks in copolymers of relatively low CL/EO ratio. Also, for similar CL/EO, the shorter the PEG segment, the stronger the impact on the crystallinity. It is worth mentioning that thermograms showed one single endothermic peak without shoulders,

Table 1
Different PCL–PEG–PCL block copolymers synthesized by MAPS.

PCL–PEG–PCL copolymer	CL/EO molar ratio[a]	M_n[a] (Da)	M_n[b] (Da)	M_w[b] (Da)	PDI[b]	CMC (10^{-6} M)
1050–6000–1050	0.14	8,100	12,250	13,400	1.10	39
1450–6000–1450	0.19	8,900	11,000	15,200	1.38	6.7
2550–6000–2550	0.33	11,100	13,000	15,000	1.16	4.7
1300–10000–1300	0.10	12,600	15,400	16,950	1.10	12
2600–10000–2600	0.20	15,200	16,700	19,700	1.18	7.4
3700–10000–3700	0.29	17,400	18,300	23,200	1.27	3.7
4500–10000–4500	0.35	19,000	16,000	19,000	1.19	2.2
1500–20000–1500	0.06	23,000	21,600	25,950	1.20	5.7
3800–20000–3800	0.15	27,600	21,600	26,200	1.21	4.7
7850–20000–7850	0.30	35,700	24,850	26,850	1.08	2.8

[a] Calculated by ^{1}H NMR.
[b] Calculated by GPC.

Table 3
Size and size distribution data of RIF-free polymeric micelles over 1 week.

PCL–PEG–PCL copolymer	Concentration (% w/v)	Time (days)	Peak 1[a]		Peak 2[b]		PDI (±S.D.)
			d_h (nm) (±S.D.)	%	d_h (nm) (±S.D.)	%	
1050–6000–1050	1	0	66.7 (3.2)	100.0	–	–	0.30 (0.02)
		1	45.6 (2.5)	20.0	590.8 (15.9)	80.0	0.73 (0.005)
		2	58.6 (6.7)	20.0	618.6 (15.7)	80.0	0.71 (0.05)
		7	52.4 (7.5)	16.0	633.4 (38.2)	84.0	0.66 (0.01)
	4	0	115.5 (10.3)	100.0	–	–	0.31 (0.06)
		1	746.5 (52.8)	68.6	4552.7 (268.2)	31.4	0.64 (0.09)
		2	125.6 (13.9)	41.4	1099.7(154.6)	58.6	0.93 (0.07)
		7	410.67 (83.9)	35.0	2590.5 (357.1)	65.0	0.80 (0.18)
1450–6000–1450	1	0	54.5(2.8)	100.0	–	–	0.21 (0.01)
		1	50.5 (2.7)	49.5	1345.3 (428.4)	50.5	0.74 (0.07)
		2	56.2 (1.8)	47.1	2057.0 (470.2)	52.9	0.83 (0.00)
		7	59.5 (19.5)	46.7	2170.7 (174.0)	53.3	0.92 (0.09)
	4	0	88.1 (0.3)	100.0	–	–	0.28 (0.01)
		1	85.4 (1.3)	71.9	1418.7 (156.5)	28.1	0.62 (0.00)
		2	94.6 (13.0)	49.8	2335.5 (565.3)	50.2	0.78 (0.04)
		7	341.6 (304.1)	44.7	2201.4 (661.5)	45.3	0.88 (0.02)
2550–6000–2550	1	0	51.2 (0.6)	100.0	–	–	0.11 (0.00)
		1	53.2 (1.1)	100.0	–	–	0.12 (0.01)
		2	55.8 (1.3)	100.0	–	–	0.20 (0.00)
		7	59.9 (3.9)	72.2	788.8(44.3)	27.8	0.53 (0.05)
	4	0	70.0 (1.7)	100.0	–	–	0.21 (0.01)
		1	74.1 (2.3)	100.0	–	–	0.23 (0.00)
		2	76.4 (1.1)	100.0	–	–	0.28 (0.01)
		7	100.8 (18.4)	65.6	2015.6 (1335.0)	34.4	0.58 (0.01)
1300–10000–1300	1	0	86.8 (4.5)	100.0	–	–	0.24 (0.01)
		1	118.5 (42.9)	78.1	2649.7 (384.0)	21.9	0.55 (0.02)
		2	84.8 (16.5)	59.8	2142.0 (154.1)	40.2	0.69 (0.02)
		7	79.1 (2.0)	48.5	930.2 (130.6)	51.5	0.75 (0.08)
	4	0	220.7 (8.1)	100.0	–	–	0.38 (0.05)
		1	243.7 (29.3)	84.4	4109.7 (820.6)	15.6	0.45 (0.03)
		2	224.0 (23.7)	66.0	3913.0 (546.5)	34.0	0.66 (0.05)
		7	354.1 (447.0)	61.7	3906.0 (248.1)	38.3	0.68 (0.06)
2600–10000–2600	1	0	79.1 (5.3)	100.0	–	–	0.21 (0.01)
		1	85.0 (8.5)	100.0	–	–	0.33 (0.01)
		2	71.3 (3.8)	69.3	593.8 (182.3)	30.7	0.41 (0.03)
		7	105.5 (11.0)	57.4	717.1(110.3)	42.6	0.75 (0.01)
	4	0	229.0 (10.2)	100.0	–	–	0.46 (0.01)
		1	222.1 (4.4)	87.9	4260.0 (279.0)	12.1	0.48 (0.02)
		2	237.1 (71.5)	84.5	3915.3 (758.4)	15.5	0.66 (0.02)
		7	214.1 (14.8)	52.3	3448.7 (236.7)	47.7	0.82 (0.05)
3700–10000–3700	1	0	84.4 (5.0)	100.0	–	–	0.21 (0.01)
		1	112.2 (5.5)	100.0	–	–	0.28 (0.01)
		2	114.8 (5.4)	100.0	–	–	0.28 (0.00)
		7	112.6 (5.6)	100.0	–	–	0.30 (0.02)
	4	0	219.1 (13.2)	100.0	–	–	0.44 (0.01)
		1	20.2 (1.5)	4.8	247.1 (19.0)	95.2	0.47 (0.01)
		2	37.1 (3.7)	14.0	226.9 (15.4)	86.0	0.46 (0.03)
		7	330.9 (71.9)	100.0	–	–	0.48 (0.00)
4500–10000–4500	1	0	90.1(2.4)	100.0	–	–	0.23 (0.01)
		1	94.9 (4.0)	100.0	–	–	0.19 (0.02)
		2	95.5 (4.8)	100.0	–	–	0.22 (0.01)
		7	108.7 (10.9)	100.0	–	–	0.26 (0.00)
	4	0	193.7 (2.3)	100.0	–	–	0.30 (0.01)
		1	207.5 (3.2)	100.0	–	–	0.30 (0.01)
		2	39.0 (6.8)	90.5	213.0 (12.9)	9.5	0.30 (0.01)
		7	254.2 (14.4)	100.0	–	–	0.33 (0.01)
1500–20000–1500	1	0	249.5 (30.8)	100.0	–	–	0.22 (0.03)
		1	170.1 (35.3)	43.0	889.5 (182.4)	57.0	0.48 (0.03)
		2	225.5 (101.1)	67.8	1174.5(431.8)	32.2	0.48 (0.01)
		7	607.1 (47.9)	78.3	1079.7(274.1)	21.7	0.42 (0.01)
	4	0	466.8 (12.5)	100.0	–	–	0.07 (0.03)
		1	498.8 (12.6)	100.0	–	–	0.08 (0.04)
		2	605.5 (126.8)	100.0	–	–	0.12 (0.06)
		7	648.8 (64.4)	100.0	–	–	0.15 (0.03)

Table 3 (*Continued*)

PCL–PEG–PCL copolymer	Concentration (% w/v)	Time (days)	Peak 1[a]		Peak 2[b]		PDI (±S.D.)
			d_h (nm) (±S.D.)	%	d_h (nm) (±S.D.)	%	
3800–20000–3800	1	0	212.3 (15.0)	100.0	–	–	0.39 (0.01)
		1	134.5 (17.1)	48.8	1012.3 (291.9)	51.2	0.64 (0.09)
		2	161.5 (40.3)	31.3	1818.0(237.2)	68.7	0.84 (0.05)
		7	149.6 (13.4)	48.8	1533.7 (387.9)/4359.8 (593.3)[c]	31.7/19.5[c]	0.83 (0.06)
	4	0	646.3 (15.8)	100.0	–	–	0.41 (0.06)
		1	496.6 (151.9)	100.0	–	–	0.50 (0.08)
		2	370.1 (20.7)	100.0	–	–	0.42 (0.12)
		7	471.6 (109.7)	100.0	–	–	0.72 (0.09)
7850–20000–7850	1	0	128.8 (1.3)	100.0	–	–	0.18 (0.01)
		1	134.4 (6.7)	100.0	–	–	0.22 (0.01)
		2	130.4 (3.8)	100.0	–	–	0.25 (0.01)
		7	127.7 (6.7)	87.4	2563.3 (171.5)	12.6	0.33 (0.01)
	4	0	431.7 (150.5)	100.0	–	–	0.26 (0.01)
		1	515.9 (37.4)	100.0	–	–	0.27 (0.01)
		2	420.8 (56.6)	100.0	–	–	0.22 (0.03)
		7	503.9 (53.5)	100.0	–	–	0.29 (0.01)

[a] Peak 1 corresponds to the fraction of smaller size.
[b] Peak 2 corresponds to the fraction of larger size.
[c] Two secondary size populations were found.

suggesting the absence of secondary crystal populations. The crystallization of PCL could not be established. On the other hand, PEG is water-soluble and the crystallization tendency of PCL in the micelles is expected to increase, this phenomenon being stronger for longer PCL segments.

3.3. Critical micellar concentration (CMC)

The drug encapsulation capacity of polymeric amphiphiles is enhanced substantially above the CMC [43]. To determine the CMC of the different copolymers, the surface tension was plotted *versus* the concentration and established as the copolymer concentration above which the surface tension displayed a less sharp change [44]. CMC values ranged between 10^{-5} and 10^{-6} M (Table 1). The higher the CL/EO ratio of the copolymer, the lower the CMC found. For example, 3700–10000–3700 (CL/EO = 0.29) and 1300–10000–1300 (CL/EO = 0.10) displayed values of 3.7×10^{-6} and 12×10^{-6} M, respectively. For similar CL/EO ratios, the higher the molecular weight of the copolymer, the greater the self-assembly tendency and the lower the CMC; e.g., 7850–20000–7850 (CL/EO = 0.30), a copolymer with CL/EO very similar to 3700–10000–3700 was 2.8×10^{-6} M. This behavior was even more remarkable when 1050-6000–1050 (CL/EO = 0.14) and 3800–20000–3800 (CL/EO = 0.15) were compared, CMC values being 39 and 4.7×10^{-6} M, respectively. It is also worth stressing that a highly hydrophilic copolymer with CL/EO as low as 0.06 (1500–20000–1500) showed a very low CMC value (5.7×10^{-6}M) that assures micellization even under extremely diluted conditions.

3.4. Copolymer solubility in water

As opposed to PEO–PPO amphiphiles, PEG–PCL copolymers usually display low aqueous solubility (<10%). This behavior relies on the especially high hydrophobicity of PCL. In general, previous works that described the preparation of drug-loaded PEG–PCL micelles assumed total copolymer solubilization [45,46]. However, the copolymer concentration used was, often, <1%. On the other hand, since higher copolymer concentrations enable the solubilization of greater drug amounts, there is an interest to increase the copolymer concentration in the system. To improve the solubility of the copolymers (and potentially the RIF solubilized amounts), PCL–PEG–PCL triblocks of decreasing CL/EO ratio were synthesized. On the contrary, greater copolymer hydrophilicity might decrease the ability to incorporate RIF (due to relatively smaller cores). To assess the intrinsic aqueous solubility of the copolymers, increasing copolymer amounts were solubilized and the final copolymer concentration estimated gravimetrically. In general, when solutions with theoretical copolymer concentrations between 1 and 4% (w/v) were prepared, more than 90% of the copolymer remained in solution. In some cases, also 6% solutions showed this relatively high solubility extent. More concentrated systems (>6%) showed a sharper decrease in the solubilized percentage to 80% (Fig. 2). The solubility loss could be associated with the insolubilization of more hydrophobic copolymer fractions displaying shorter PEG and longer PCL blocks. These results confirm that the experimental solubility of these biomaterials needs to be assayed before one proceeds to drug solubilization studies. Otherwise, the real copolymer concentration could be overestimated. Based on these data, RIF solubilization studies were conducted with micellar suspensions of up to 4–6% (w/v) (see below).

3.5. Preparation and characterization of RIF-free micelles

The size, size distribution, and zeta potential of different drug-free 1 and 4% micellar suspensions were characterized by DLS (Table 3). At day 0, 1 and 4% micelles showed unimodal size distributions. 1% PEG6000 micelles ranged between 51.2 and 66.7 nm for 2550–6000–2550 and 1050–6000–1050, respectively; PDI values were between 0.11 and 0.31. 4% systems also showed a unimodal pattern, though larger aggregates were observed (70.0–115.5 nm). The larger size of 1050–6000–1050 micelles (CL/EO = 0.14) would probably stem from (i) the more hydrophilic nature of the copolymer (containing very short PCL blocks with lower micellization tendency) and the preferential generation of inter-chain PCL associations (over intra-chain ones) and (ii) a less condensed core [47]. Aiming to confirm that PCL–PEG–PCL triblocks form larger micelles than MPEG–PCL diblocks of similar composition, a 5000–5150 diblock ($M_{n\mathrm{NMR}}$ = 10,150 Da, CL/EO = 0.40) was synthesized and the aggregation behavior was characterized. The d_h of 4% 5000–5150 micelles was 56.1 nm, in full agreement with previous results [48,49]. In contrast, 4% 2550–6000–2550 micelles, a derivative displaying similar M_n and CL/EO, showed larger micelles of 70.0 nm. 1% PEG10000 micelles displayed sizes of approximately 80–90 nm, the length of PCL blocks showing a minimal effect on the size. 4% PEG10000 systems formed much larger aggregates (193.7–229.0 nm). Micellar enlargement was

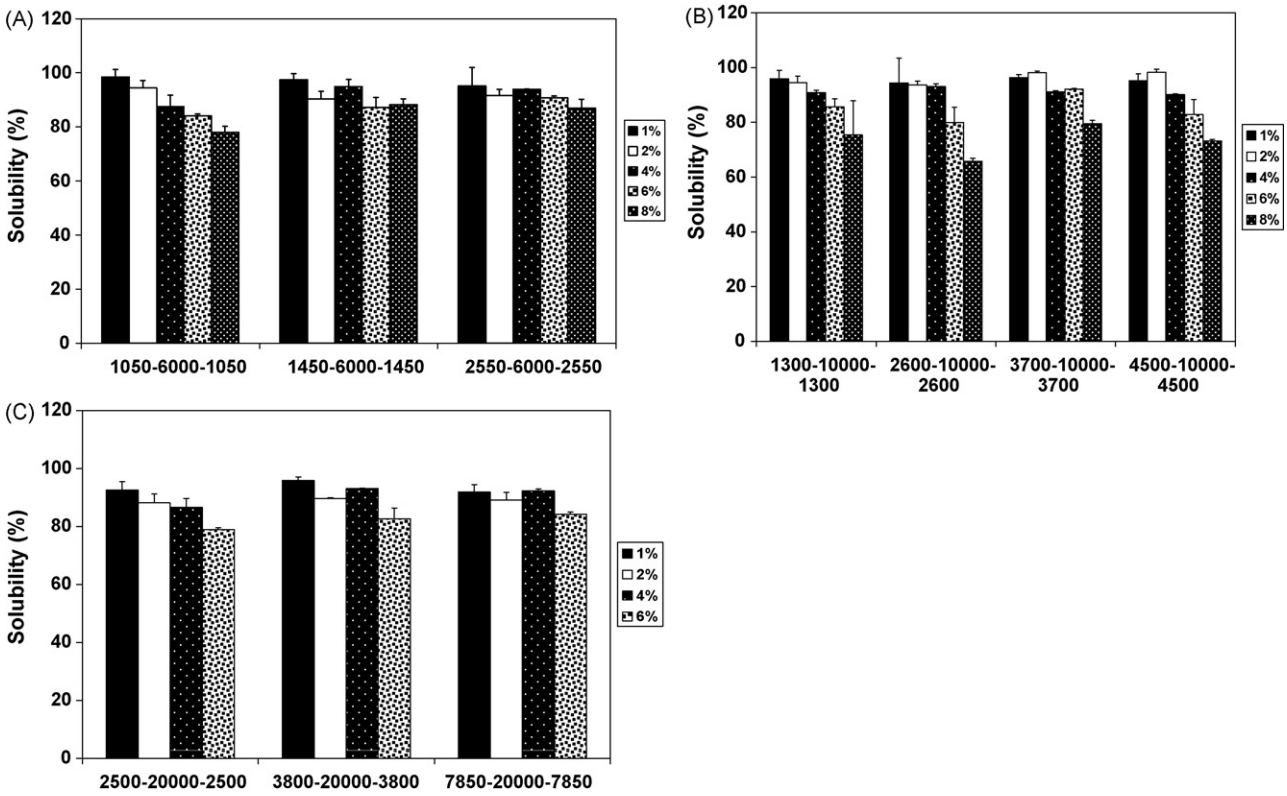

Fig. 2. Solubility of the different PCL–PEG–PCL copolymers in water expressed as the percentage of copolymer (%) remaining in solution for increasing theoretical copolymer concentrations.

even more pronounced in 1% PEG20000-made micelles probably due to the greater hydrophilic central block; the shorter the PCL block (and lower CL/EO ratios), the larger the size found. For example, 1500–20000–1500 and 7850–20000–7850 showed d_h values of 249.5 and 128.9 nm, respectively. This behavior was similar to that of PEG6000 derivatives and also suggested the generation of strong inter-chain associations for copolymers with low CL/EO ratios. 4% PEG20000 systems displayed a dramatic size growth with initial sizes in the 430–650 nm range. These data stressed the high tendency of larger molecules to undergo phase separation, regardless of the CL/EO ratio. Overall DLS data confirmed that the molecular weight of the central PEG segment is a key structural feature determining the initial size of the aggregates; e.g., 1% 3700–10000–3700 and 3800–20000–3800 (similar PCL block) displayed sizes of 84.4 and 212.3 nm, respectively. The effect of the hydrophobic component was less marked, especially for more diluted systems. The generation of sub-micron particles was favored at greater copolymer concentrations, where more densely packed micellar systems are generated and stronger inter-chain interactions are favored.

Table 4
RIF solubility factors (f_s) in PCL–PEG–PCL micelles.

PCL–PEG–PCL copolymer	Concentration (% w/v)	RIF solubility factors (f_s) (±S.D.)
1050–6000–1050	1	0.75 (0.02)
	4	1.53 (0.02)
1450–6000–1450	1	0.80 (0.02)
	4	1.58 (0.04)
2550–6000–2550	1	0.83 (0.02)
	4	1.78 (0.11)
1300–10000–1300	1	1.88 (0.01)
	4	4.01 (0.04)
	6	5.18 (0.18)
2600–10000–2600	1	1.95 (0.00)
	4	4.05 (0.06)
	6	5.37 (0.22)
3700–10000–3700	1	1.99 (0.01)
	4	4.10 (0.05)
	6	5.39 (0.19)
4500–10000–4500	1	2.02 (0.01)
	4	4.23 (0.09)
	6	5.43 (0.18)
1500–20000–1500	1	0.74 (0.01)
	4	1.01 (0.01)
3800–20000–3800	1	0.79 (0.02)
	4	1.35 (0.09)
7850–20000–7850	1	1.10 (0.02)
	4	1.38 (0.03)

Zeta potential measurements showed that the surface of the nano-aggregates is almost neutral, independently of the copolymer composition and molecular weight; values ranged between −2.28 and 0.55 mV. The morphology of the micelles was characterized by TEM. Results are exemplified for 4% 3700–10000–3700 in Fig. 3. Micelles were spherical and showed variable sizes, though water evaporation during sample preparation and shrinkage of the structures could lead to size underestimation. Conversely, the inclusion of hydration water molecules in the calculation of the average hydrodynamic diameter by DLS overestimates their dimensions. Considering these facts, results with both techniques fitted very well.

3.6. Physical stability of RIF-free micelles

PEG-PCL-based micelles show low stability in water and undergo gradual secondary aggregation and size growth over time [50]. This behavior results in fast copolymer (and drug) precipitation. In general, drug-loaded PCL–PEG–PCL systems are

Table 5
Size and size distribution data of RIF-loaded polymeric micelles over 1 week.

PCL–PEG–PCL copolymer	Concentration (% w/v)	Time (days)	Peak 1[a]		Peak 2[b]		PDI (±S.D.)
			d_h (nm) (±S.D.)	%	d_h (nm) (±S.D.)	%	
1050–6000–1050	1	0	59.8 (2.9)	100.0	–	–	0.22 (0.00)
		1	180.2 (9.1)	100.0	–	–	0.32 (0.02)
		2	248.7 (5.3)	100.0	–	–	0.33 (0.03)
		7	247.5 (20.5)	100.0	–	–	0.18 (0.02)
	4	0	132.8 (27.6)	100.0	–	–	0.34 (0.05)
		1	98.0 (12.1)	46.8	772.5 (97.6)	53.2	0.74 (0.08)
		2	125.6 (13.9)	47.4	1099.7 (154.6)	52.6	0.91 (0.09)
		7	472.6 (25.8)	96.6	4918 (183.0)	4.3	0.33 (0.04)
1450–6000–1450	1	0	54.4 (3.3)	100.0	–	–	0.21 (0.00)
		1	68.9 (10.2)	83.0	322.3 (65.1)	17.0	0.40 (0.02)
		2	56.2 (10.6)	63.8	451.2 (13.1)	36.2	0.57 (0.08)
		7	400.2 (29.9)	100.0	–	–	0.40 (0.00)
	4	0	123.8 (2.2)	100.0	–	–	0.42 (0.02)
		1	121.2 (2.8)	59.6	575.1 (86.8)	40.4	0.54 (0.05)
		2	115.2 (10.7)	67.3	994.9 (106.2)	32.7	0.56 (0.12)
		7	70.07 (10.0)	15.9	1430 (321.6)	84.1	0.73 (0.24)
2550–6000–2550	1	0	68.6 (0.8)	100.0	–	–	0.15 (0.01)
		1	70.2 (1.1)	100.0	–	–	0.17 (0.00)
		2	72.2 (2.2)	100.0	–	–	0.18 (0.01)
		7	93.1 (4.4)	100.0	–	–	0.29 (0.04)
	4	0	111.6 (3.0)	100.0	–	–	0.25 (0.01)
		1	108.0 (4.8)	100.0	–	–	0.25 (0.01)
		2	113.6 (0.8)	100.0	–	–	0.26 (0.00)
		7	122.8 (0.45)	100.0	–	–	0.36 (0.02)
1300–10000–1300	1	0	62.3 (0.6)	100.0	–	–	0.18 (0.01)
		1	98.2 (54.3)	72.0	289.8 (46.0)	28.0	0.42 (0.02)
		2	112.5 (34.6)	100.0	–	–	0.33 (0.08)
		7	275.3 (31.8)	100.0	–		0.08 (0.07)
	4	0	299.8 (8.7)	100.0	–	–	0.50 (0.03)
		1	258.8 (7.4)	94.8	4510.0 (408.3)	5.2	0.43 (0.02)
		2	217.5 (55.3)	80.9	4157.3 (155.8)	19.1	0.50 (0.10)
		7	83.92 (6.75)	93.1	3687.8 (472.1)	6.9	0.31 (0.02)
2600–10000–2600	1	0	77.7 (2.8)	100.0	–	–	0.29 (0.01)
		1	81.1 (1.4)	83.5	1220.7 (31.5)/ 4036.0 (174.5)	8.5/8.0[c]	0.42 (0.01)
		2	77.4 (16.4)	65.2	564.7 (100.3)/ 4624.0 (323.7)[c]	25.2/9.6[c]	0.59 (0.05)
		7	104.0 (26.7)	65.9	732.5 (97.4)/ 4711.0 (437.1)[c]	18.3/15.8[c]	0.47 (0.01)
	4	0	200.5 (2.1)	100.0	–	–	0.36 (0.05)
		1	250.9 (9.3)	47.8	1307.7 (164.7)/ 4289.7 (320.4)[c]	29.8/22.4[c]	0.70 (0.04)
		2	818.7 (41.7)	49.5	3364.3 (336.5)	50.5	0.53 (0.04)
		7	629.8 (244.7)	68.2	3394.0 (1354.8)	32.8	0.73 (0.20)
3700–10000–3700	1	0	75.4 (11.0)	100.0	–	–	0.22 (0.01)
		1	159.1 (15.4)	100.0	–	–	0.39 (0.01)
		2	46.9 (6.0)	28.8	265.5 (56.3)	71.2	0.45 (0.04)
		7	301.5 (25.5)	100.0	–	–	0.29 (0.01)
	4	0	148.3 (12.1)	100.0	–	–	0.33 (0.03)
		1	154.2 (1.0)	100.0	–	–	0.30 (0.00)
		2	147.3 (7.1)	100.0	–	–	0.30 (0.01)
		7	142.3 (9.9)	100.0	–	–	0.34 (0.04)
4500–10000–4500	1	0	34.4 (20.0)	10.6	183.1 (4.7)	89.4	0.29 (0.01)
		1	263.3 (11.9)	100.0	–	–	0.22 (0.01)
		2	255.0 (13.0)	100.0	–	–	0.17 (0.03)
		7	255.0 (10.1)	100.0	–	–	0.05 (0.02)
	4	0	152.3 (7.8)	100.0	–	–	0.33 (0.05)
		1	128.1 (13.0)	100.0	–	–	0.27 (0.00)
		2	140.1 (5.8)	100.0	–	–	0.42 (0.06)
		7	126.9 (8.6)	100.0	–	–	0.32 (0.04)
1500–20000–1500	1	0	153.9 (26.8)	100.0	–	–	0.35 (0.03)
		1	277.6 (22.2)	100.0	–	–	0.12 (0.02)
		2	291.2 (22.8)	100.0	–	–	0.12 (0.02)
		7	358.7 (16.6)	100.0	–	–	0.07 (0.04)
	4	0	540.6 (14.7)	100.0	–	–	0.08 (0.02)
		1	599.4 (86.2)	100.0	–	–	0.29 (0.03)
		2	758.6 (50.4)	100.0	–	–	0.12 (0.07)
		7	966.3 (100.5)	100.0	–	–	0.19 (0.04)

Table 5 (*Continued*)

PCL–PEG–PCL copolymer	Concentration (% w/v)	Time (days)	Peak 1[a]		Peak 2[b]		PDI (±S.D.)
			d_h (nm) (±S.D.)	%	d_h (nm) (±S.D.)	%	
3800–20000–3800	1	0	132.7 (19.9)	100.0	–	–	0.31 (0.06)
		1	67.9 (22.2)	12.1	416.3 (79.8)	87.9	0.39 (0.08)
		2	367.6 (19.5)	100.0	–	–	0.22 (0.03)
		7	443.5 (57.8)	100.0	–	–	0.27 (0.02)
	4	0	1397.8 (137.2)	100.0	–	–	0.51 (0.04)
		1	2600.7 (431.4)	100.0	–	–	0.56 (0.04)
		2	928.6 (158.0)	100.0	–	–	0.31 (0.03)
		7	1083 (803.0)	85.8	4390 (719.2)	14.2	0.57 (0.07)
7850–20000–7850	1	0	119.0 (2.9)	100.0	–	–	0.16 (0.01)
		1	124.5 (9.8)	100.0	–	–	0.20 (0.00)
		2	122.0 (7.6)	100.0	–	–	0.22 (0.01)
		7	135.9 (11.2)	76.1	921.5 (91.2)	23.9	0.48 (0.23)
	4	0	574.8 (37.6)	100.0	–	–	0.28 (0.02)
		1	510.6 (40.1)	100.0	–	–	0.28 (0.01)
		2	540.2 (32.4)	100.0	–	–	0.28 (0.01)
		7	498.4 (57.1)	100.0	–	–	0.32 (0.03)

[a] Peak 1 corresponds to the fraction of smaller size.
[b] Peak 2 corresponds to the fraction of larger size.
[c] Two secondary size populations were found.

freeze–dried immediately after preparation trying to preserve their initial size, though they usually display a substantial size growth. To study the influence of the copolymer structure on the physical stability and the consequent change in micellar size over time, drug-free 1 and 4% micellar suspensions were stored at 25 °C and the size, the size distribution and the zeta potential were followed up. In general, the size of the aggregates gradually increased. Also, the appearance of more than one size population was observed. Copolymers of greater molecular weight and CL/EO >0.20 were more stable than more hydrophilic copolymers (<0.20) of low molecular weight (Table 3). PEG6000 derivatives showed the lowest stability and the most pronounced size growth of all the series under investigation. This behavior was accelerated in more concentrated systems. For example, 1050–6000–1050 and 1450–6000–1450 generated microparticles even at day 1, while 2550–6000–2550 micelles were slightly more stable (Table 3). 4% systems of PEG10000 copolymers with short PCL segments (e.g., 1300–10000–1300 and 2600–10000–2600) also showed a fast size growth. As previously shown, the initial size of PCL–PEG–PCL micelles, as determined by DLS, is mainly governed by the size of the hydrophilic PEG segment (Table 3). In this context, PEG20000 micelles displaying a larger corona showed the highest steric stabilization properties and the less pronounced size growth over time. On the other hand, secondary aggregation stems from the interaction and fusion of hydrophobic domains of different copolymer molecules. However, PCL segments need to be sufficiently long and mainly in an amorphous state to fuse; highly crystalline PCL domains fuse more slowly [51]. PCL blocks of intermediate length do not crystallize fast enough to prevent fusion, though they are sufficiently long to undergo gradual inter-molecular fusion, generating much larger aggregates at day 2; fused PCL probably crystallize at later time points, stabilizing the super-aggregates. In contrast, micelles of copolymers with longer PCL blocks are more prone to crystallize rapidly upon preparation, generating more stable nanoparticles owing to the prevention of the fusion process from the beginning. This is the case of 1 and 4% 3700–10000–3700 and 4500–10000–4500 micelles that showed relatively high stability as expressed by the minor size change. A similar trend was found for PEG20000 derivatives, 1500–20000–1500 being the less stable one. It is worth mentioning though, that these copolymers initially formed aggregates of much greater initial size. Zeta potential data did not show substantial changes (not shown).

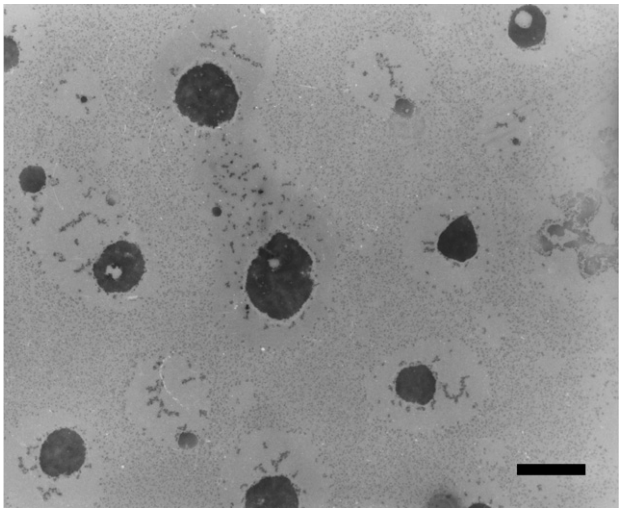

Fig. 3. TEM micrograph of RIF-free 4% 3700–10000–3700 micelles prepared in water and negatively stained with 2% uranyl acetate. Scale bar = 100 nm.

3.7. Encapsulation of RIF

Investigating the encapsulation of RIF within PCL–PEG–PCL micelles and establishing the main molecular parameters ruling this process was a central goal of this work. First, the influence of the time of addition of the copolymer/RIF acetone solution to the aqueous phase on the encapsulation efficiency was tested for 6% 3700–10000–3700 micelles. The more prolonged the addition time, the greater the encapsulated amount of RIF; e.g., S_a values were 11.5 ± 0.7 ($f_s = 4.49$), 13.8 ± 0.7 ($f_s = 5.39$), 15.5 ± 1.2 ($f_s = 6.05$) and 16.1 ± 1.6 ($f_s = 6.29$) mg/mL, respectively, for addition times of 10, 20, 30 and 40 min. Data at 20, 30 and 40 min were not significantly different. On the other hand, the higher the RIF load attained, the lower the physical stability of the system. To find the equilibrium between encapsulation efficiency, stability and preparation time, in advance, an addition time of 20 min was used. 1% PEG6000 micelles showed f_s values ≤ 1 (S_a is lower than the intrinsic solubility), indicating the deleterious interaction between both amphiphiles (copolymer and drug). Following a similar trend, 4% systems improved the aqueous solubility of RIF to less than 2 times (Table 4); e.g., 4% 1050–6000–1050, 1450–6000–1450 and

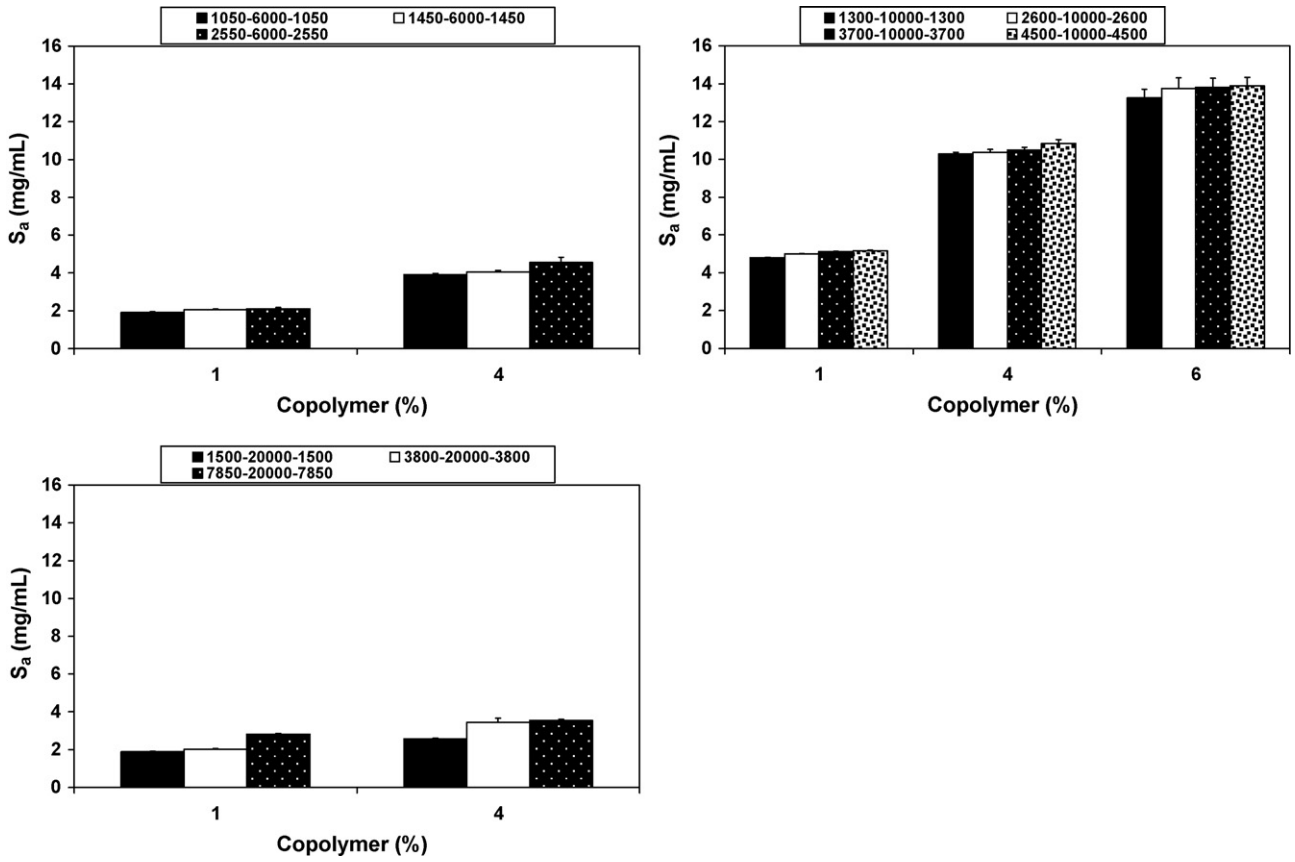

Fig. 4. Apparent solubility (S_a) of RIF in the different PCL–PEG–PCL micellar systems.

2550–6000–2550 showed S_a values of 3.92, 4.05 and 4.56 mg/mL (Fig. 4), representing f_s of 1.53, 1.58 and 1.78, respectively. In spite of the larger size of 4% 1050–6000–1050 micelles (115.5 nm) compared to the other PEG6000 derivatives, this copolymer displays the shortest PCL blocks (and the smallest core) and, thus, the lowest encapsulation capacity of the series (Table 4). This behavior suggested that RIF is mainly hosted within the hydrophobic domain; note the slight increase in the solubility in copolymers with greater CL/EO ratio. In addition, the size increase attained with 2550–6000–2550 with respect to 5000–5150 micelles led to a minor encapsulation improvement. Copolymers bearing longer PEG and PCL blocks (and forming larger micelles with larger cores) showed better encapsulation efficiency. For example, S_a values for 4% 1300–10000–1300, 2600–10000–2600, 3700–10000–3700 and 4500–10000–4500 were 10.27, 10.36, 10.50 and 10.83 mg/mL, respectively (Fig. 4); these values represent solubility improvements of 4.01, 4.05, 4.10 and 4.23 times (Table 4). 6% systems showed an even higher solubilization capacity (up to 5.43-fold). A further concentration increase led to a sharp loss in copolymer solubility and a decrease in the RIF solubilization due to the formation of macroscopic RIF/copolymer adducts and the fast precipitation of the copolymer and the drug.

Despite the larger size shown in DLS analysis, PEG20000 micelles did not incorporate RIF efficiently. S_a values were 1.89, 2.02 and 2.82 mg/mL for 1% 1500–20000–1500, 3800–20000–3800 and 7850–20000–7850, respectively (Fig. 4). This behavior stemmed from the fact that the size growth was mainly due to a larger corona that usually stabilizes the aggregate but does not improve the solubilization capacity of the micelle. More concentrated micelles showed an extremely slight increase in the solubilization capacity (Fig. 4). The encapsulation process depends on two key parameters: (i) drug-micelle affinity and (ii) micelle physical stability. PEG10000 and PEG20000 copolymers of similar CL/EO ratios are expected to display similar affinity for the drug. However, to maintain CL/EO ratios comparable to those of the other series, PEG20000 amphiphiles bear longer PCL segments with higher crystallization tendency and lower solubility in water. It is also worth stressing that PEG20000 itself displays a lower solubility in water than PEG10000. To maintain RIF in solution, copolymers need to remain soluble. Our results indicated that RIF-loaded PEG20000 systems were less stable and precipitated rapidly

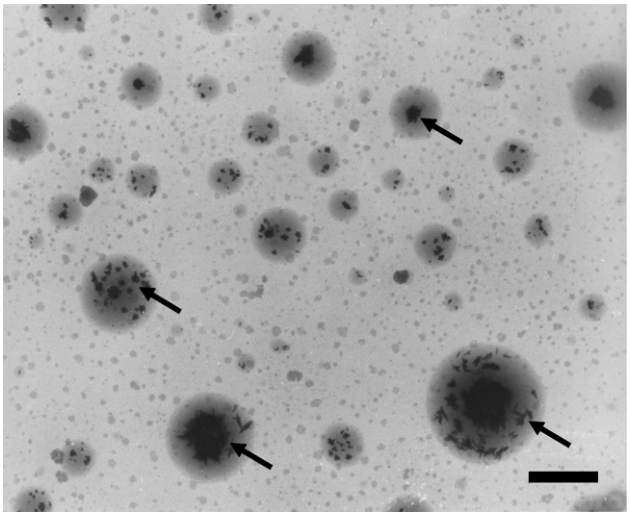

Fig. 5. TEM micrograph of RIF-loaded 4% 3700–10000–3700 micelles prepared in water and negatively stained with 2% uranyl acetate. Arrows point out RIF crystals within the micelles. Scale bar = 100 nm.

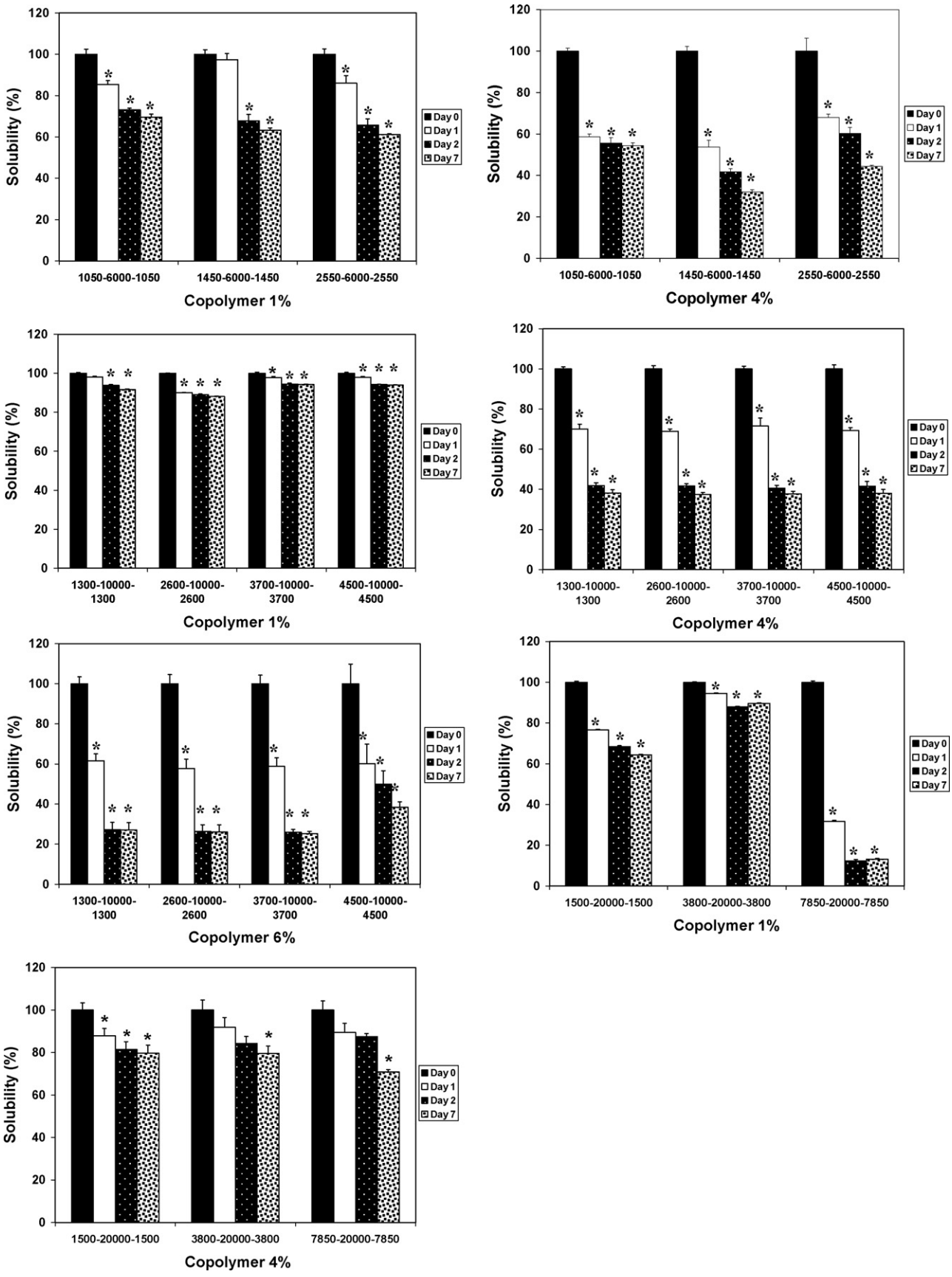

Fig. 6. RIF concentration in solution (%) of drug-loaded polymeric micelles stored at 25 °C, over 1 week. '*' Statistically significant decrease ($p < 0.05$) of the RIF concentration when compared to the initial RIF concentration of the system.

during preparation, thus resulting in micelles with much lower encapsulation capacity, regardless of the larger size. Moreover, solutions of PEG20000 copolymers were also substantially more viscous, displaying gel-like characteristics even at copolymer concentrations as low as 1% that hindered the solubilization process [48]. In summary, PEG10000 micelles appear to show the optimal equilibrium between micellar size and polymer solubility, leading to the best encapsulation capacity.

Overall data confirmed that the micellar size (determined by the molecular weight of PEG) is the main structural feature governing the encapsulation of RIF. The contribution of the PCL length to the solubilization capacity for identical PEG is less marked. On the other hand, extremely long hydrophobic segments (introduced to balance the CL/EO ratio of copolymers with larger PEG) lead to remarkable lower micellar solubility as clearly observed with PEG20000 micelles. It is worth stressing that the solubilization extents found with PEG10000 micelles are higher than those reported for RIF/CD complexes [25–27] and mannosylated dendrimers [28].

3.8. Characterization of RIF-loaded micelles

The size and the size distribution of the drug-loaded nanoparticles is a key parameter in the interaction with different cell types and may dictate the fate of the nanocarriers *in vivo*, regardless of the administration route [52]. In the specific case of this work that envisions the oral administration of the systems, the gastrointestinal absorption strongly depends on the size of the particles [52]. Drug incorporation into the micellar core could also change the aggregation pattern and the stability of the aggregates. In general, drug-loaded micelles display enlarged sizes due to (i) the expansion of the micellar core [53] or (ii) the fusion of drug-containing micelles into larger ones [54]. The former leads to a slight to moderate size growth, while the latter usually to more dramatic size changes. It could also change the aggregation pattern and the physical stability of the aggregates. The especially high molecular weight of RIF and its dual amphoteric/amphiphilic nature make the prediction of the interaction with the micelles very difficult. At day 0, samples showed a unimodal aggregation. 1% micelles of highly hydrophilic copolymers (CL/EO <0.15) underwent a clear size decrease upon RIF encapsulation with respect to drug-free micelles (Table 5): e.g., 1500–20000–1500 (CL/EO = 0.06), 1050–6000–1050 (CL/EO = 0.14), 3800–20000–3800 (CL/EO = 0.15) decreased from 249.5, 66.7 and 212.3 nm to 153.9, 59.8 and 132.7 nm, respectively. These findings would suggest the formation of micelles of lower aggregation number. Conversely, 1% micelles of more highly hydrophobic amphiphiles (CL/EO >0.33) showed a clear size growth. Copolymers with intermediate CL/EO values (0.19–0.30) remained almost unchanged. The analysis of RIF-containing 4% systems is less straightforward. Most of the samples showed a clear size increase with respect to the drug-free counterpart. For example, PEG6000 micelles with PCL blocks of 1050, 1450 and 2550 Da expanded from 115.5, 88.0 and 70.0 nm to 132.8, 123.8 and 111.6 nm, respectively. PEG20000 copolymers showed a similar trend. The size growth would be consistent with the enlargement of the core upon RIF solubilization. In contrast, PEG10000 micelles showed a different behavior. For example, 1300–10000–1300 (CL/EO = 0.10) showed a clear size increment from 220.7 to 299.8 nm upon RIF incorporation, while more hydrophobic derivatives displayed aggregates of smaller size; e.g., 4500–10000–4500 decreased from 193.7 to 152.3 nm. Overall findings indicate that (i) RIF disturbs the aggregation process of PCL–PEG–PCL, (ii) the RIF/micelle interaction and the resulting micellar size are intimately associated not only with the CL/EO ratio but also with the PCL length and (iii) micellar fusion is presumably being promoted by the drug in copolymers of sufficiently long PCL blocks, this phenomenon being more favored at higher copolymer concentrations. Despite the slightly negatively charged character of RIF at pH 5.8 [55], its incorporation into the micelles did not affect the surface properties and zeta potential values remained almost unchanged (not shown). These results suggest that the drug remains mainly associated to the micellar core (Table 5) and were supported by TEM analysis, where RIF crystals were clearly visualized within the micelles (Fig. 5); drug crystals were probably generated during the drying process.

3.9. Physical stability of RIF-containing micelles

To gain further insight into the influence of RIF incorporation on the physical stability of the micelles, the concentration of RIF and the size and size distribution of drug-loaded micelles was investigated over 1 week. In general, 1% 10,000 systems were physically stable, the remaining percentage of RIF in solution being >90%, at day 7 (Fig. 6); differences were statistically significant owing to the very small S.D. found. In contrast, 1% PEG6000 systems were less stable and RIF concentrations were between 60 and 70%, at day 7. It is worth noting that these systems displayed S_a values lower than the intrinsic solubility in water. 4% PEG6000 were also instable, percentages being 54, 31 and 44% for copolymers with PCL blocks of 1050, 1450 and 2550 Da, at day 7. PEG20000 followed a similar trend, 3800–20000–3800 being the most stable of this series, regardless of the concentration. More concentrated dispersions often displayed a sharper concentration loss. For example, the concentrations of RIF in 6% PEG10000 micelles decreased to approximately 60% at day 1, while 4% systems only to 70%. Later on, a sharper decrease was apparent. It should be stressed though, that 4500–10000–4500 micelles were the most stable of this series, probably due to the more effective stabilization of the micellar core and the prevention of micellar fusion.

DLS measurements showed a steady size growth over time and the appearance of more than one size fraction. This phenomenon was more pronounced for more concentrated systems of copolymers with lower molecular weight and relatively low to intermediate CL/EO ratio (CL/EO <0.2) such as 1050–6000–1050, 1450–6000–1450, 1300–10000–1300 and 2600–10000–2600 (Table 5). These size changes were accompanied by the increase of the polydispersity. Data strongly support the destabilization of the micelles by the encapsulated RIF presumably due to the inability of these copolymers to stabilize the micellar core by PCL crystallization. Copolymers of the same families, though with greater CL/EO values were much more stable (e.g., 2550–6000–2550, 3700–10000–3700 and 4500–10000–4500). Interestingly, some samples presented two size fractions at intermediate time points (e.g., 1% 3700–10000–3700 at day 2) that converge into one single population later on. This phenomenon suggests that a dynamic process of micellar disassembly and re-aggregation might be taking place to generate relatively more stable systems. Regardless of the very low CL/EO value, 4% 1500–20000–1500 showed a more controlled size increase from 540.6 nm at day 0 to 966.3 nm at day 7. Finally, a comprehensive analysis of the solubilization and stability data indicates that copolymers combining relatively large PEG central blocks with high CL/EO display the best combination of encapsulation capacity and stability over time.

4. Conclusions

The design of novel anti-TB antibiotics is one of the rationales currently followed to address resistant strains of the mycobacterium, to shorten the treatment course and to minimize drug interactions with other anti-TB and anti-HIV drugs. Alternatively,

if managed appropriately, first generation anti-TB drugs still show good effectiveness. Nanotechnologies appear as one of the most promising approaches to overcome main technological limitations (e.g., poor aqueous solubility and stability), to increase patient compliance and adherence to the regimens and to target bacterial reservoirs (e.g., alveolar macrophages) [56]. On the other hand, TB is an infection mainly striking poor populations in developing countries and, in this particular situation, making these innovative medicines affordable to all the patients is another challenge [57].

In the present work, we aimed to more deeply understand the structural parameters governing the RIF encapsulation within PCL–PEG–PCL flower-like polymeric micelles; this drug is one of the most potent and effective anti-TB ones. The micellar size appears as the most crucial property, this phenomenon being primarily controlled by the molecular weight of the PEG central block. Sufficiently high CL/EO ratios (and long PCL segments) are also demanded to attain relatively physically stable micellar systems with cores that are large enough to host the bulky RIF molecule. PEG10000 micelles with CL/EO ratios >0.30 combine the best encapsulation capacity and the highest physical stability of all the amphiphiles investigated. Having expressed this, the freeze–drying of drug-loaded systems appears, at this stage, mandatory to assure their physical stability in the long-term range. In this context, the use of cryo-protectants is probably also required [58]. Based on the size profile displayed, RIF-loaded micelles of these biocompatible copolymers could fulfil the demands for the administration by the oral route. It is also worth stressing that a new administration route is emerging in TB: pulmonary local delivery [56]. In this context, RIF-loaded micelles might also represent a valuable alternative to other nano- and micron-sized carriers. However, a priori, the goal is to evaluate the pharmacokinetic performance after the oral administration. Ongoing experiments are focused on the investigation of the chemical stability of the encapsulated RIF in a broad range of pH values and in contact with INH and of its oral bioavailability.

Acknowledgements

RJG and MAM thank Ph.D. scholarships of the CONICET. DAC and AS are members of the CONICET. The authors thank Dr. L. Diaz and Dr. G. Copello (Faculty of Pharmacy and Biochemistry, University of Buenos Aires) and Dr. G. Abraham (INTEMA, National University of Mar del Plata, Argentina) for GC and GPC analysis, respectively.

References

[1] S.H. Kaufmann, A.J. McMichael, Nat. Med. 11 (2005) S33.
[2] Tuberculosis. The International Union Against Tuberculosis and Lung Disease. http://www.theunion.org/tuberculosis/tuberculosis.html (accessed February 2008).
[3] I. Smith, Clin. Microb. Rev. 16 (2003) 463.
[4] M.P. Golden, H.R. Vikram, Am. Family Phys. 72 (2005) 1761.
[5] T.R. Frieden, T.R. Sterling, S.S. Munsiff, C.J. Watt, C. Dye, Lancet 362 (2003) 887.
[6] Global tuberculosis control: surveillance, planning, financing, WHO report 2008. http://www.who.int/tb/publications/global_report/2008/pdf/fullreport.pdf (accessed February 2008).
[7] S.K. Jain, G. Lamichhane, S. Nimmagadda, M.G. Pomper, W.R. Bishai, Microbe 3 (2008) 285.
[8] World Health Organization, Sozial- und Präventivmedizin 38 (1993) 251.
[9] P. Onyebujoh, A. Zumla, I. Ribeiro, R. Rustomjee, P. Mwaba, M. Gomes, J.M. Grange, Bull. World Health Organ. 83 (2005) 857.
[10] WHO, Treatment of tuberculosis: guidelines for national programmes, 3rd Geneva World Health Organization, 2003.
[11] C. Dye, Lancet 367 (2006) 938.
[12] T. Brewer, S. Heymann, Arch. Med. Res. 36 (2005) 617.
[13] E.C. Rivers, R.L. Mancera, Drug Discov. Today 13 (2008) 1090.
[14] C. Becker, J.B. Dressman, H.E. Junginger, S. Kopp, K.K. Midha, V.P. Shah, S. Stavchansky, D.M. Barends, J. Pharm. Sci. 98 (2009) 2252.
[15] S. Agrawal, R. Panchagnula, Int. J. Pharm. 287 (2004) 97.
[16] M. Zaru, S. Mourtas, P. Klepetsanis, A.M. Fadda, S.G. Antimisiaris, Eur. J. Pharm. Biopharm. 67 (2007) 655.
[17] T.T. Mariappan, S. Singh, Int. J. Tuberc. Lung Dis. 7 (2003) 797.
[18] T.T. Mariappan, S. Singh, Clin. Res. Reg. Affairs 23 (2006) 1.
[19] C.J. Shishoo, S.A. Shah, I.S. Rathod, S.S. Savale, J.S. Kotecha, P.B. Shah, Int. J. Pharm. 190 (1999) 109.
[20] S. Singh, T.T. Mariappan, N. Sharda, S. Kumar, A.K. Chakrabarti, Pharm. Pharmacol. Commun. 6 (2000) 405.
[21] C.J. Shishoo, S.A. Shah, I.S. Rathod, S.S. Savale, M.J. Vora, Int. J. Pharm. 228 (2001) 53.
[22] M.C. Gohel, K.G. Sarvaiya, AAPS PharmSci.Tech. 8 (2007), Article 68.
[23] G.G. Gallo, P. Radaelli, in: K. Florey (Ed.), Analytical Profiles of Drug Substances, vol. 5, Academic Press, Inc., Orlando, FL, USA, 1976, p. 467.
[24] N. Maggi, A. Vigevani, G.G. Gallo, C.R. Pasqualucci, J. Med. Chem. 11 (1968) 936.
[25] D.A. Ferreira, A.G. Ferreira, L. Vizzotto, A. Federman Neto, A. Gomes de Oliveira, Braz. J. Pharm. Sci. 40 (2004) 43.
[26] S.K. Mehta, K.K. Bhasin, N. Mehta, S. Dham, Colloid Polym. Sci. 283 (2005) 532.
[27] B. Prakash Rao, S. Sarasija, C. Narendra, Balasangameshwer, Ars Pharm. 47 (2006) 37.
[28] P. Vijayaraj Kumar, A. Asthana, T. Dutta, N.K. Jain, J. Drug Target 14 (2006) 546.
[29] A. Sosnik, A. Carcaboso, D.A. Chiappetta, Recent Pat. Biomed. Eng. 1 (2008) 43.
[30] D.A. Chiappetta, A. Sosnik, Eur. J. Pharm. Biopharm. 66 (2007) 303.
[31] J. Gonzalez-Lopez, C. Alvarez-Lorenzo, P. Taboada, A. Sosnik, I. Sandez-Macho, A. Concheiro, Langmuir 24 (2008) 10688.
[32] L. Piao, Z. Dai, M. Deng, X. Chen, X. Jing, Polymer 44 (2003) 2025.
[33] W.-J. Lin, L.-W. Juang, Ch-Ch. Lin, Pharm. Res. 20 (2003) 668.
[34] M.A. Moretton, R.J. Glisoni, D.A. Chiappetta, A. Sosnik, BIOOMAT 2009, I Workshop on Artificial Organs, Biomaterials and Tissue Engineering, Latin American Society of Biomaterials, Tissue Engineering and Artificial Organs (SLABO), Rosario, Argentina, August 2009.
[35] Y. Yang, C. Hua, Ch.M. Dong, Biomacromolecules 10 (2009) 2310.
[36] G. Gotelli, G.A. Abraham, A. Sosnik, ARCHIPOL 2009-V Argentine-Chilean Polymer Symposium, Los Cocos, Córdoba, Argentina, October 2009, 2009.
[37] C.O. Kappe, Angew. Chem. Int. Ed. 43 (2004) 6250.
[38] European Pharmacopeia 3rd Edition, Supplement, Council of Europe (2000) 298.
[39] A.R. Rote, A.K. Sharma, Int. J. Pharm. 59 (1997) 119.
[40] G. Schwach, M. Vert, Int. J. Biol. Macromol. 25 (1999) 283.
[41] A. Sosnik, D. Cohn, Polymer 44 (2003) 7033.
[42] P.J. Sánchez-Soto, J.M. Ginés, M.J. Arias, C.S. Novák, A. Ruiz-Conde, J. Therm. Anal. Calorim. 67 (2002) 189.
[43] J. Dong, J. Armstrong, B.Z. Chowdry, S.A. Leharne, Therm. Acta 417 (2004) 201.
[44] J. Dong, B.Z. Chowdry, S.A. Leharne, Colloids Surf. A 24 (2004) 91.
[45] M. Laird Forrest, J.A. Yáñez, C.M. Remsberg, Y. Ohgami, G.S. Kwon, N.M. Davies, Pharm. Res. 25 (2008) 194.
[46] K. Letchford, R. Liggins, K.M. Wasan, H. Burt, Eur. J. Pharm. Biopharm. 71 (2009) 196.
[47] Y. Zhao, H. Liang, S. Wang, C. Wu, J. Phys. Chem. B 105 (2001) 848.
[48] K. Letchford, R. Liggins, H. Burt, J. Pharm. Sci. 97 (2008) 1179.
[49] J. Liu, F. Zeng, C. Allen, Eur. J. Pharm. Biopharm. 65 (2007) 309.
[50] Y. Hu, Y. Ding, Y. Li, X. Jiang, Ch. Yang, Y. Yang, J. Nanosci. Nanotech. 6 (2006) 3032.
[51] G. Gaucher, M.-H. Dufresne, V.P. Sant, N. Kang, D. Maysinger, J.-C. Leroux, J Control Release 109 (2005) 169.
[52] A.V. Kabanov, I.R. Nazarova, I.V. Astafieva, E.V. Batrakova, V.Y. Alakhov, A.A. Yaroslavov, V.A. Kabanov, Macromolecules 28 (1995) 2303.
[53] D.A. Chiappetta, C. Hocht, C. Taira, A. Sosnik, Nanomedicine 5 (2010) 11.
[54] D.A. Chiappetta, J. Degrossi, S. Teves, M. DïAquino, C. Bregni, A. Sosnik, Eur. J. Pharm. Biopharm. 69 (2008) 535.
[55] N. Changsan, A. Nilkaeo, P. Pungrassami, T. Srichana, J. Drug Target 17 (2009) 751.
[56] A. Sosnik, A.M. Carcaboso, R.J. Glisoni, M.A. Moretton, D.A. Chiappetta, Adv. Drug Del. Rev. 62 (2010) 547.
[57] A. Sosnik, M. Amiji, Adv. Drug Del. Rev. 62 (2010) 365.
[58] A. Richter, C. Olbrich, M. Krause, J. Hoffmann, T. Kissel, Eur. J Pharm. Biopharm. (2010), doi:10.1016/j.ejpb.2010.02.010.